L JAST
Libya Journal Applied For Science and Technology
مجلة ليبيا للعلوم التطبيقية والتقنية
Volume 5.Issue1
December2018

Effects of Treatment Time on Formation of PEO Coatings on Regular Shape Aluminium Foil Substrates

Husein Meshreghi[1], Aleksey Yerokhin[2]
[1]Chemical Technology Engineering, Sok Alkhamis Imsehel High Tec. Institute, Tripoli, Libya
[2]Material Science and Engineering, University of Manchester, Manchester, United Kingdom

Abstract

Over the last decade, thick and thin alumina films have been actively studied and their fabrication by conventional methods such as tape casting has grown significantly due to their applications as substrates dielectric. However, some defects such as cracks may appear essential for the manufacture using, caused by use of certain additives on the surfaces. Plasma electrolytic oxidation (PEO) is a surface engineering technique that converts the surface of light metals and alloys into oxide ceramics layers. This work is based on the application of PEO process on Al-foil 50 µm with different treatment times. For better understanding of the conversion process the produced alumina has been studied in different sample regions. The alumina created by PEO technique was characterized in terms of thickness distribution, porosity, roughness and phase composition using scanning electronic microscope and x-ray diffraction. The effect of the degree of conversion of the aluminium into oxide was studied and possible limitations to create uniform alumina layers on the inner surfaces and edges of complex shapes were discussed.

Keywords: Plasma electrolyte oxidation, Conversion, Alumina,

1. Introduction

One of the important variables needs to be taken into consideration during creation of a PEO coating is the time of the process. The time affects the morphology and thickness of the PEO coatings, which change the coating characteristics [1, 2]. Therefore, the oxidation time for PEO treatment should be investigated and optimized.

Different treatment times varying from a few minutes to several of hours have been used in research to understand characteristics and properties of the formed coatings [3-6]. The thickness and morphology of the coatings are affected primarily, which can change the properties. Commonly, increasing the treatment time results in thicker coatings produced under more powerful and larger micro-discharges causing bigger discharge channels in the oxide layer as reported by Sundararajan et. al.[2]. However, this increase in thickness may have different effect on coating behaviour. Dun Lee et. al and Hussein et. al. [7, 8] reported a linear dependence of the coating thickness on treatment time, whilst non-linear behaviour was reported by Al Bosta et. al. [1]. Treatment time of the PEO process not only influences oxide layer thickness
but also surface roughness. The linear increase in coating roughness is directly related to the fact that the mean average diameter of discharge channels also increases linearly with coating time. Crystalline phases such as γ- and α-alumina formed during the PEO process are strongly affected by volcano-like features and the accumulated particles in the coating, which in turn is influenced by the treatment time, and this is consistent with the results reported by Yerokhin et. al [5]. The main objectives of this work of are: (i) to analyse the effect of PEO processing time on the characteristics and properties of the coatings deposited in different regions of a regular shape aluminium foil substrates; (ii) estimate the coatings growth efficiency during PEO processes (ii) find out the acceptable PEO processing time to get a relatively high degree of conversion of Al into its oxide and the limitations to create uniform coatings on the surface substrates.

2. Experimental set-up

Rectangular samples of aluminium foil (0.05% Mg; 0.05% Mn; 0.25% Si; 0.07%Zn; 0.4%Fe; and Al balance) with dimensions of 30 mm × 15 mm × 0.05 mm and surface roughness of Ra ≈ 0.1- 0.2 µm were used. The exposed working area of the samples measured using a vernier calliper was 4.5 cm2. The experimental setup is shown in (fig 1). The PEO rig consisted of a 30 KW power unit and a 2-L stainless steel tank equipped with magnetic stirring and cooling by continuous pumping via cold water heat exchanger to maintain the temperature between 25 to 35 oC.

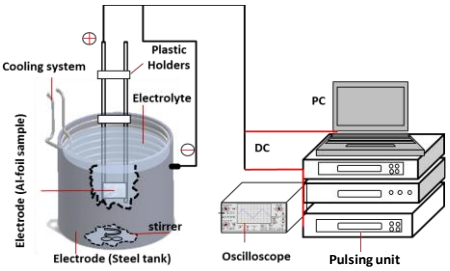

Fig. 1 Schematic of PEO processing equipment.

3. Results and discussion

3.1 Characterization of current density during PEO

The current density–time response for the PEO coatings produced for various treatment times are shown in (fig 2).

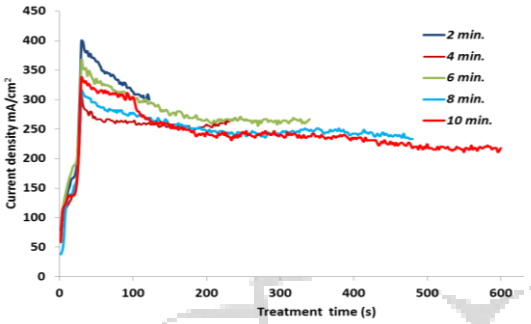

Fig. 2 The plot of current density versus PEO treatment time

At the first stage, an initial linear increase in current density occurred through a short period of time to values from 0.32 A/cm2 to 0.4 A/cm2 based on the ramp time setting up for the voltage raise to the pre-set values, which are 530 V and -120 V in our work. Before the required voltage is reached, there were similarities in the shape of curves for all conditions, whatever the current density value is reached. This rising is similar to the creation of the conventional anodic oxidation as well as the thin aluminium oxide film. This appears to be similar to the results in references [1, 9-13]. This stage is controlled by the hydrogen and oxygen reactions products over the working electrode surface, which means the increasing of current is limited by a partial shielding action of hydrogen and oxygen [5]. A comparison of the curves showed no considerable difference in current density behaviour during the treatments for 6, 8 and 10 min. However, the maximum value achieved in the sample treated for 2 min process time due to the lower electrical resistance gaseous vapour envelope. At this point, the electric field strength on coating reaches the maximum value, which is sufficient to initiate ionisation phenomena at the electrode-electrolyte interface. This corresponds to the breakdown voltage of the oxide film formed on the specimen surface. Then, the current density slowly reduces with time. The major change occurs during the first 160 to 170 s as can be seen in the curves of samples treated for 6, 8 and 10 min. This indicates that the coating thickness changes considerably during this period of time. During the 4-min treatment, it took around 70 sec to reach the steady state, while the sample treated for 2 min did not reach it at all. The duration of this period depends on the critical thickness of oxide film, which in turn depends on the values of current. In our work the treatments were carried out at constant voltages, however the current density varied for different samples.

3.2 Thickness measurements

The thicknesses of coatings formed in both sides at different regions on the working electrodes is shown in (fig 3).

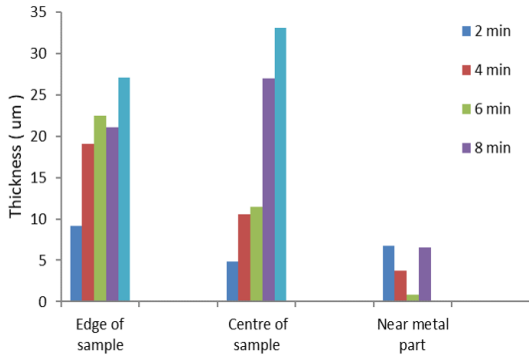

Fig. 3 The PEO coating thickness as a function of treatment time in the edge region, at the centre region and near the metal part

Figure 3 shows the thickness of the PEO coatings in the centre and edge regions is often a linear function of the treatment time and the data shows it is possible to obtain coatings with thickness more than 32 µm at one side in the central region. It can be noticed that, as the treatment time of the PEO process increases the coating thickness increases too. This relation between the thickness and treatment time is consistent with the observations by Dunleavy et. al.[9], who conducted PEO treatment of an aluminium alloy in a similar electrolyte. To compare the coating thickness between the three regions, the thicker oxide films under all treatment conditions were formed in the edge regions, except samples processed for 8 and 10 min, where the coatings in the central region were slightly thicker than at the edge. Figure 4 shows the oxide growth rate at different process times. As can be seen in (fig 4 & 5) the growth rate of the oxide layer formed for 2 min was 0.04 µm/sec and it continues increasing until reaching around 0.06 µm/sec for the coating formed for 8 min. After that the growth rate decreases to 0.05 µm/sec for the coating formed for 10 min.

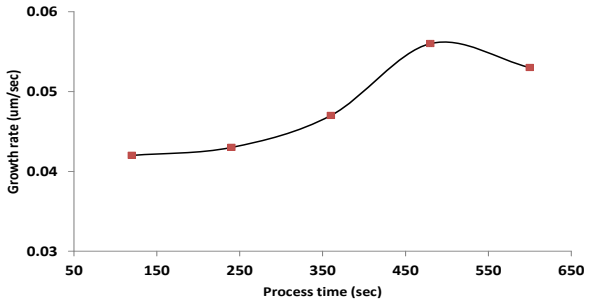

Fig. 4 Coating growth rate at different treatment times (side A)

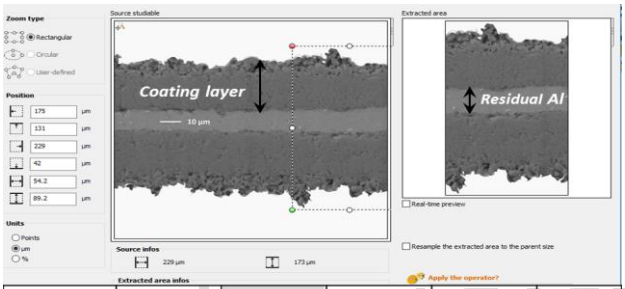

Treatment time (min)	2	4	6	8	10
Residual Al thickness (µm)	47.5	37.5	30	12	10

Fig. 5 SEM images of a cross section of PEO coating on Al foil treated for 10 min, showing residual aluminium thickness.

Hussein et. al. [8] in discussing the ceramic layer growth mechanism during the PEO treatment stated that the oxide layer grows inwards and outwards concurrently. However during the first stages, the oxide layer grows mainly outwards and after a certain thickness is reached the growth towards the substrate becomes faster.

In order to achieve a better understanding about the mechanism of the coating formation and the conversion of Al to alumina, the treatment time was increased to 12 min to achieve the full conversion to alumina. The total thickness of the resulting oxide layer was 75 ± 1.5 µm and the full conversion to alumina occurred except for a small area not exceeding 1.0 % from the total area of bulk material (aluminium foil) distributed in different area along the sample length as shown in (fig 6).

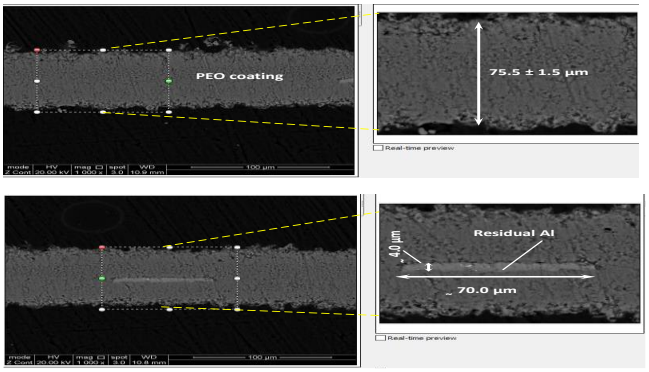

Fig. 6 SEM micrographs of cross-sections of PEO coatings on the sample treated for 12 min showing full conversion and a small area of residual aluminium.

3.3 SEM morphologies

Figure 7 presents the SEM micrographs of surface morphology of oxide coatings in different regions of Al foil samples treated for different periods of time. All samples showed a number of "pancake" like features, with discharge pores of irregular shape were located on the coating surface, which is a common feature of PEO coatings. In central regions of the samples treated for 6 and 8 min, a centre of each pancake featured a pore formed by the discharge channel through which the molten aluminium surged out, reacted with oxygen and quickly solidified leaving pores and distinct boundaries [1, 14]. In the sample treated for 6 min, the size of the pores in the central region ranged from 3 to 6 □m, with some areas on the surface occupied by volcano-like structures created by discrete localised micro-discharge events. The volcano-like features indicate the surface temperature during the PEO process was high, which explains the high strength of the microdischarges [2, 15, 16]. Relatively large holes in the centre of the pancake for all samples suggested that there were strong localized discharges and such holes penetrate in the coating thickness. As shown in (fig 7), some microcracks exist in the coating at the central region of the sample treated for 8 min, as indicated by the white circle. This is maybe due to the temperature difference between the coating and the electrolyte, which is caused by the rapid cooling. During the PEO treatment the temperature in the discharge channels was very high, reaching thousands degrees Celsius, and the electrolyte temperature ranged from 30 to 40 oC rate. Therefore, subsequent thermal shocks led to the appearance of cracks in the oxide layer [14, 17].

SEM micrographs in (fig 8) show cross-sectional morphology of the coatings formed in different regions of aluminium foil samples at different processing times. For all samples, the oxide layers appeared to have a

significant amount of porosity, holes, and discharge channels within the coating and near the coating substrate interface, in all sample regions. Such defects and porosity were likely to be caused by powerful discharges developed at the sample surface. During the PEO coating growth, the porosity was formed as a result of localized oxygen trapping in molten aluminium in the vicinity of plasma discharges. So it will possible that the pore network helps the creation of relatively high thickness oxide layers by allowing the electrolyte to penetrate deep into the growing layer during the treatment [18].

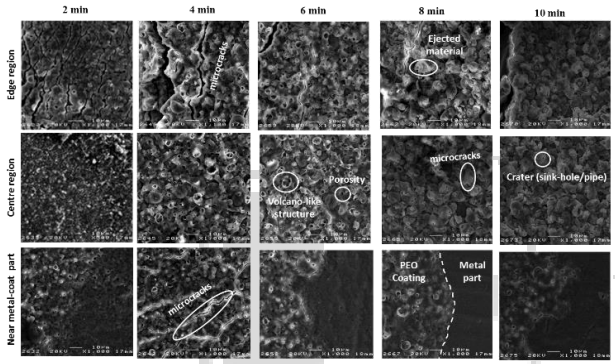

Figure .7 SEM micrographs of surface morphology of oxide films in different regions at different treatment times.

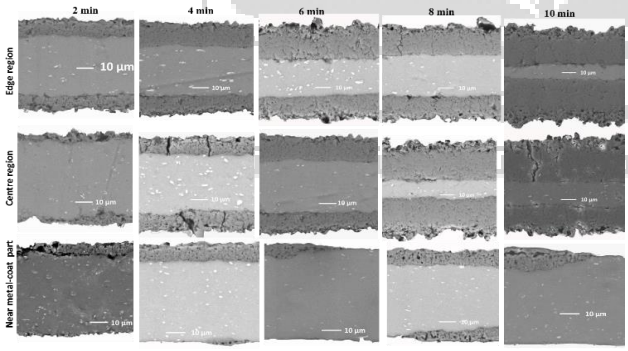

Figure .8 SEM micrographs of cross-sectional morphology of oxide films formed in different regions and for different periods of time.

The software MountainsMap 7.2 was used to estimate the coating porosity. The highest porosity was present in the edge region in the sample treated for 2 min. While the sample treated for 10 min was characterised by lowest porosity in both regions. Thus porosity decreased steadily with processing time.

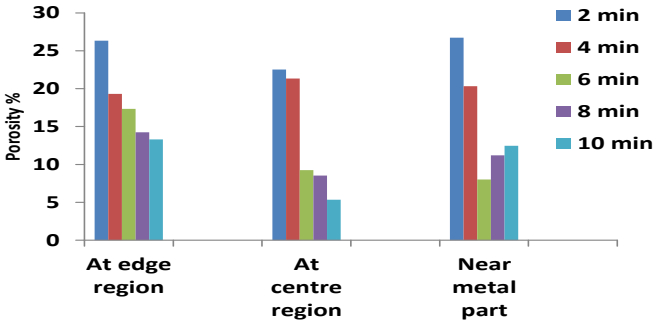

Figure. 9 PEO coating porosity in different regions of the sample.

Percentage of surface porosity of PEO coatings in edge, central and near metal part regions of Al foils formed at different treatment times is shown in (fig. 9). The results obtained indicate that the morphology of oxide films on aluminium foil produced by the PEO process in different regions is significantly different. It can be seen clearly that the porosity at the edges was found to be greater than that at the central region, however in both regions the percentage of porosity on the surface decreases with increase the treatment time.

There is strong correlation between the mechanical properties of the PEO coatings and their structure [19, 20]. Porosity can effect on the coating properties, such as hardness, dielectric strength and corrosion resistance. For the lowest porosity, the highest coating hardness, chemical stability and dielectric strength can be expected. However, the combination of good coating adhesion with surface-connected porosity provided by moderated surface roughness confers good tribological performance of PEO coatings in many applications.

Surface roughness is important parameter that may influence the characteristics of morphology. Krishna et. al. in his study of the tribological performance of ultra-hard ceramic coatings states that the surface roughness of the PEO coatings is a linear function of the final coating thickness [21]. An increase in processing time provides adequate opportunity for the build-up of the PEO coating, which leads to an increase in the coating thickness. However with an increase in treatment time, the discharges become more energetic and violent, which causes the formation of non-uniform coatings with higher roughness [22]. The results of surface roughness (Rz) analysis are shown in (fig. 10), indicating that the surface roughness increased with the increasing processing time.

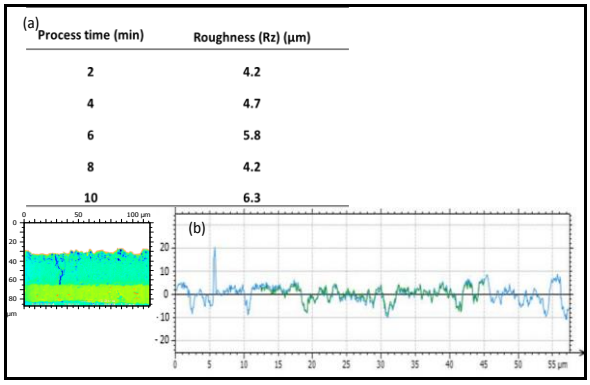

Figure. 10 (a) The surface roughness values in the central region of PEO coatings produced at different processing times and (b) an example of corresponding line scan profile of surface roughness on the Al foil sample PEO treated for 10 min.

3.4 Phase composition analysis

Figure 11 displays X-ray diffraction patterns of ceramic coatings on the samples treated for 6, 8 and 10 min.

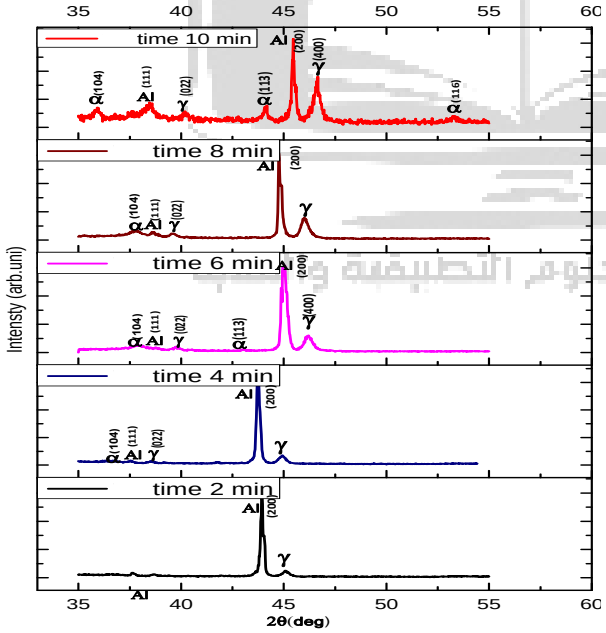

Fig. 11 XRD pattern of PEO coatings produced for different process times

From positions of diffraction peaks, the phases were identified by comparison with the reference pattern of γ-Al2O3 (PDF# 50-0741), α- Al2O3 (PDF# 46-1212) and Al substrate (PDF# 04-0787) [23, 24].

Analysis of the diffraction patterns indicates that all studied PEO coatings are mainly composed of γ-Al2O3 and α-Al2O3 the ratio of which characterised by the heights of (400)γ and (113)α peaks located at 46.2o and 43.1o 2θ comprises approximately 6:1, 7:1 and 5:2 for the samples treated for 6, 8 and 10 min respectively. It is found that the intensity of (200)Al peak at 45.10o 2θ decreases as the treatment time increases. However, the highest intensity of (113)α peak is observed in the sample treated in 10 min. These phase profiles resemble those previously reported by Sundararajan et al [2], Xue et al [25], and Guangliang et al [20].

3.5 Evaluation of oxide film growth efficiency during PEO process

Usually, during anodising the current density consists of i_i is the ionic current of the oxide film growth, i_d is the anodic dissolution current and i_e is the current caused by oxygen evolution. In research paper published by Bakovets et. al. [26] the current efficiency in PEO process of Al in electrolyte solution 40 g/l Na2O.3SiO3 for treatment time 6 min was 9.1%. Yerokhin et. al. [27] evaluated the current efficiency for the partial processes of oxide film formation, dissolution and oxygen evolution in the PEO process of Al in aqueous solutions of KOH with 0.5-2.0 g/l. In this work, the estimations of the PEO process efficiency for the coatings formed in different treatment times are carried out assuming that current yields of the partial processes of oxide layer growth ($\eta_{Al_2O_3}$), dissolution ($\eta_{Al_{sol}}$) and gas evolution (η_{O_2}) on the surface of working electrode are dominated by the Faraday's law. So, on the anode surface the balance equation for the current yields of the partial processes can be written as follows [27]:

$$\eta_{Al_2O_3} + \eta_{Al_{sol}} + \eta_{O_2} = 100\% \quad (1)$$

In our results, the effect of treatment time on the coating thickness is obvious, where the oxide film thickness increases with increasing the treatment time (fig. 3). To assist the optimisation of the process efficiency, the current efficiency of the partial electrode processes during the PEO treatment was evaluated for different treatment times. The calculated values and processing parameters are presented in table 1.

Treatment time (min)	Charge, Q_{tot} (C)	Coating thickness, (µm)	Al lost, m_{Al}^{sol} (g)
2	425.4	10.0	0.1215×10^{-2}
4	728.5	20.0	8×10^{-3}
6	1036.8	32	0.122×10^{-1}
8	1285.5	52	0.023
10	1291.4	64	0.024

Table 1 Coating thicknesses, dissolved Al and total charge of PEO process in 1 g l-1 KOH, 2 g L-1 Na2SiO3, and 2 g L-1 Na4P2O7 solution for different treatment times

Assuming the alumina density ρ = 3.1 g/cm3 and based on reference data given in table 4 the results of current efficiency for the products of partial anodic processes in PEO of process of aluminium foil in different treatment times presented in (fig 12).

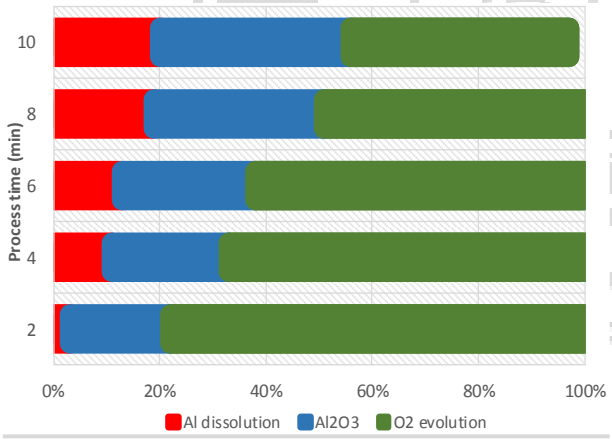

Fig. 12 Current efficiency for partial anodic processes in PEO process of Al foil for different process time

From (fig. 19) it can be seen that the current efficiency of the oxide layer growth ranges from 19-36 %, increasing with treatment time. Similarly, the aluminium loss increases with treatment time. Although the current efficiency of oxygen evolution decreases with time, the fraction of total current spent on the oxygen evolution is always more than a half of the total current for all conditions, i.e. oxygen evolution remains the dominant electrochemical process.

Conclusions

1. The results indicated that the oxide layer thickness increases with increasing in treatment time. However in the last stage, the coating growth rate was reduced due to the anodic dissolution and recrystallisation of the coating.
2. By the treatment for 12 min with resulted in the coating thickness of 75 ± 1.5 µm, complete conversion of aluminium foil into alumina was successfully achieved, except for a very small area that does not exceed 1 % of the sample volume. However such sample showed high brittleness.
3. According to the results obtained, in the central and at the edge regions the coating, porosity decreased and the surface roughness increased with treatment time. While in the near metal part of the sample, where the PEO coating only started formation, these characteristics showed a non-linear behaviour. The pore size distribution analysis indicated that the pores are mainly smaller than 6 µm under all treatment conditions. However the results in coating of sample treated for 6 min having a more uniformly distributed porosity with smaller pore size.
4. Treatment time affected the gamma to alpha alumina transformation. Both γ and α - alumina are observed after 6 min varying in relative proportion through the coating thickness. However in coating on the sample treated for 4 min composed almost only of gamma alumina.

References

[1] M. M. S. Al Bosta, K.-J. Ma, and H.-H. Chien, "The effect of MAO processing time on surface properties and low temperature infrared emissivity of ceramic coating on aluminium 6061 alloy," Infrared Physics & Technology, vol. 60, pp. 323-334, 2013.
[2] G. Sundararajan and L. Rama Krishna, "Mechanisms underlying the formation of thick alumina coatings through the MAO coating technology," Surface and Coatings Technology, vol. 167, no. 2–3, pp. 269-277, 2003.
[3] F. Jaspard-Mécuson et al., "Tailored aluminium oxide layers by bipolar current adjustment in the Plasma Electrolytic Oxidation (PEO) process," Surface and Coatings Technology, vol. 201, no. 21, pp. 8677-8682, 2007.
[4] A. I. Sonova and O. P. Terleeva, "Morphology, structure, and phase composition of microplasma coatings formed on Al-Cu-Mg alloy," Protection of Metals, journal article vol. 44, no. 1, pp. 65-75, 2008.

[5] A. L. Yerokhin, X. Nie, A. Leyland, A. Matthews, and S. J. Dowey, "Plasma electrolysis for surface engineering," Surface and Coatings Technology, 1999.
[6] C. S. Dunleavy, J. A. Curran, and T. W. Clyne, "Self-similar scaling of discharge events through PEO coatings on aluminium," Surface and Coatings Technology, vol. 206, no. 6, pp. 1051-1061, 2011.
[7] B.-H. A. Dong-Gun Lee, Uk-Rae Cho, "Effects of time variation on formation of oxide layers of Al7075 aluminum alloy by Electrolytic plasma processing (EPP)," presented at the Fracture & Strength of Solids, Jeju, Korea, 2013.
[8] R. O. Hussein, X. Nie, and D. O. Northwood, "An investigation of ceramic coating growth mechanisms in plasma electrolytic oxidation (PEO) processing," Electrochimica Acta, vol. 112, pp. 111-119, 12/1/ 2013.
[9] C. S. Dunleavy, J. A. Curran, and T. W. Clyne, "Time dependent statistics of plasma discharge parameters during bulk AC plasma electrolytic oxidation of aluminium," Applied Surface Science, vol. 268, no. 0, pp. 397-409, 2013.
[10] J. Martin et al., "Effects of electrical parameters on plasma electrolytic oxidation of aluminium," Surface and Coatings Technology, vol. 221, no. 0, pp. 70-76, 4/25/ 2013.
[11] R. O. Hussein, X. Nie, and D. O. Northwood, "An investigation of ceramic coating growth mechanisms in plasma electrolytic oxidation (PEO) processing," Electrochimica Acta, vol. 112, no. 0, pp. 111-119, 2013.
[12] C. E. V.-R. Barchiche, D. Rocca, E., "A better understanding of PEO on Mg alloys by using a simple galvanostatic electrical regime in a KOH–KF–Na3PO4 electrolyte," Surface and Coatings Technology, vol. 205, no. 17–18, pp. 4243-4248, 2011.
[13] A. L. Yerokhin et al., "Oxide ceramic coatings on aluminium alloys produced by a pulsed bipolar plasma electrolytic oxidation process," Surface and Coatings Technology, vol. 199, no. 2, pp. 150-157, 2005.
[14] K. Wang, B.-H. Koo, C.-G. Lee, Y.-J. Kim, S.-H. Lee, and E. Byon, "Effects of electrolytes variation on formation of oxide layers of 6061 Al alloys by plasma electrolytic oxidation," Transactions of Nonferrous Metals Society of China, vol. 19, no. 4, pp. 866-870, 2009.
[15] W. D. Z. L. Y. C. R. Xue, "Analysis of Phase Distribution for Ceramic Coatings Formed by Microarc Oxidation on Aluminum Alloy," (in English), JACE Journal of the American Ceramic Society, vol. 81, no. 5, pp. 1365-1368, 1998.
[16] J. A. Curran and T. W. Clyne, "Thermo-physical properties of plasma electrolytic oxide coatings on aluminium," Surface and Coatings Technology, vol. 199, no. 2–3, pp. 168-176, 2005.
[17] T. Wei, F. Yan, and J. Tian, "Characterization and wear- and corrosion-resistance of microarc oxidation ceramic coatings on aluminum alloy," Journal of Alloys and Compounds, vol. 389, no. 1–2, pp. 169-176, 2005.
[18] J. A. Curran and T. W. Clyne, "Porosity in plasma electrolytic oxide coatings," Acta Materialia, vol. 54, no. 7, pp. 1985-1993, 2006.
[19] X. L. A. S. H. W. Y. A. L. D. S. J. M. A. Nie, "Thickness effects on the mechanical properties of micro-arc discharge oxide coatings on aluminium alloys," (in English), SURFACE AND COATINGS TECHNOLOGY, vol. 116-119, no. 3, pp. 1055-1060, 1999.
[20] Y. Guangliang, L. Xianyi, B. Yizhen, C. Haifeng, and J. Zengsun, "The effects of current density on the phase composition and microstructure properties of micro-arc oxidation coating," Journal of Alloys and Compounds, vol. 345, no. 1–2, pp. 196-200, 2002.
[21] L. Rama Krishna, K. R. C. Somaraju, and G. Sundararajan, "The tribological performance of ultra-hard ceramic composite coatings obtained through microarc oxidation," Surface and Coatings Technology, vol. 163–164, no. 0, pp. 484-490, 1/30/ 2003.
[22] N. P. S. Narayanan, S. Lee, Min Ho, "Surface modification of magnesium and its alloys for biomedical applications.," (in English), 2015.
[23] "Standard transition aluminas. Electron microscopy studies," (in English), 2000.
[24] G. Lv et al., "Characteristic of ceramic coatings on aluminum by plasma electrolytic oxidation in silicate and phosphate electrolyte," Applied Surface Science, vol. 253, no. 5, pp. 2947-2952, 2006.
[25] W. Xue, Z. Deng, R. Chen, and T. Zhang, "Growth regularity of ceramic coatings formed by microarc oxidation on Al–Cu–Mg alloy," Thin Solid Films, vol. 372, no. 1–2, pp. 114-117, 2000.
[26] L. A. S. V. Chernenko, I. Papanova, "Coating by Anodic Spark Electrolysis," Khimiya, Leningrad, (in Russian, ISBN 5-7245-0588-6). 1991.
[27] A. Y. L.Snizhko, A. Pilkington, N. Gurevina, D. Misnyankin, A. Leyland , A. Matthews, "Anodic processes in plasma electrolytic oxidation of aluminium in alkaline solutions," Electrochimica Acta, vol. 49, pp. 2085-2095, 2004.